

Article

Leaching of Manganese from Marine Nodules at Room Temperature with the Use of Sulfuric Acid and the Addition of Tailings

Norman Toro ^{1,*}, Manuel Saldaña ², Jonathan Castillo ³ , Freddy Higuera ² and Roxana Acosta ⁴

¹ Departamento de Ingeniería en Metalurgia y Minas, Universidad Católica del Norte, Antofagasta 1270709, Chile

² Departamento de Ingeniería Industrial, Universidad Católica del Norte, Antofagasta 1270709, Chile; msp018@alumnos.ucn.cl (M.S.); fhiguera@ucn.cl (F.H.)

³ Departamento de Ingeniería en Metalurgia, Universidad de Atacama, Copiapó 1531772, Chile; jonathan.castillo@uda.cl

⁴ Departamento de Educación, Universidad de Antofagasta, Antofagasta 1270300, Chile; roxana.acosta@uantof.cl

* Correspondence: ntoro@ucn.cl; Tel.: +56-552651021

Received: 21 March 2019; Accepted: 9 May 2019; Published: 11 May 2019



Abstract: Based on the results obtained from a previous study investigating the dissolution of Mn from marine nodules with the use of sulfuric acid and foundry slag, a second series of experiments was carried out using tailings produced from slag flotation. The proposed approach takes advantage of the Fe present in magnetite contained in these tailings and is believed to be cost-efficient. The surface optimization methodology was used to evaluate the independent variables of time, particle size, and sulfuric acid concentration in the Mn solution. Other tests evaluated the effect of agitation speed and the MnO₂/Fe₂O₃ ratio in an acid medium. The highest Mn extraction rate of 77% was obtained with an MnO₂/Fe₂O₃ ratio of 1/2 concentration of 1 mol/L of H₂SO₄, particle size of −47 + 38 μm, and 40 min of leaching. It is concluded that higher rates of Mn extraction were obtained when tailings instead of slag were used, while future research needs to focus on determination of the optimum Fe₂O₃/MnO₂ ratio to improve dissolution of Mn from marine nodules.

Keywords: secondary products; reducing agent; waste reuse; acid media

1. Introduction

Ferromanganese (Fe–Mn) deposits are present in the oceans across the world, marine ridges, and plateaus where the currents have delivered sediments for millions of years [1]. These deposits form through the accumulation of iron and manganese oxides in seawater, within either volcanic or sedimentary rocks that act as substrates, as observed in the central and northeastern ocean beds of the Pacific [2]. They may have economic potential [3], due to the high concentrations of Co, Ni, Te, Ti, Pt, and rare earth elements [4]. These Fe–Mn oceanic deposits include ferromanganese crusts, as well as cobalt-rich crusts, polymetallic nodules, and hydrothermal infusions [5]. Polymetallic nodules have a particular importance for the steel industry as they may eventually become an alternate source of manganese [6].

In order to extract manganese and other metals from marine nodules, the use of a reducing agent is necessary [7]. Acid leaching of marine nodules, with the use of iron as a reducing agent, has shown good results [8–10]. In a previous study carried out by Toro et al. [11], several parameters were evaluated for dissolving Mn from marine nodules using slag at room temperature in an acid medium. This study established that high MnO₂/Fe₂O₃ ratios significantly shorten the manganese dissolution

time from 30 to 5 min. They also conclude that MnO₂ particle size does not significantly affect the Mn extraction rate in an acid medium in the presence of Fe contained in ferrous slag.

The positive effect of Fe as a reducing agent for dissolving Mn from marine nodules was noted when lower Mn/Fe ratios were used [8–11]. Bafghi et al. [12] and Toro et al. [11] determined that sulfuric acid concentration is less important than Fe concentration in dissolving Mn.

The Mn extraction rate increases with a higher agitation speed [13–15]. Jiang et al. [13] evaluated the kinetic aspects of manganese and silver extraction during leaching of pyrolusite in sulfuric acid solutions in the presence of H₂O₂, and concluded that agitation speed was one of the most important variables affecting the Mn extraction rate. Su et al. [14] indicated that the Mn extraction rate increases significantly when the agitation speed increases from 100 to 700 rpm because high speed improves mixing and allows better contact between reagents and reactants. Jiang et al. [13] also reported that the extraction rate decreases slightly at 1000 rpm because excessive agitation can cause material to adhere to the walls of the reactor and prevent it from being leached. Velásquez et al. [16] indicated that it is only necessary to keep particles in suspension and prevent agglomeration.

The addition of Fe as a reducing agent in temperature-controlled acid media has already been studied [8,10,12]. In particular, Zakeri et al. [10] used ferrous ions with a Fe²⁺/MnO₂ ratio of 2.4 and sulfuric acid as a leaching agent with a H₂SO₄/MnO₂ ratio of 2.0 over a temperature range of 20 to 60 °C, and found out that Mn extraction was notably higher at 60 °C and reached 96% after 60 min. Bafghi et al. [12] used Fe sponge with a molar ratio of 2, and H₂SO₄ with a molar ratio of 4 (both ratios with respect to MnO₂), under the same temperatures as Zakeri et al. [10]; at 60 °C, 100% of the Mn present within the nodules was dissolved in 3 min. Both cases demonstrate the positive impact of higher temperature on the extraction rate; however, the positive impact of the presence of iron indicated that effective processing may take place even at ambient temperatures. Furthermore, both studies demonstrate that the acid concentration is less significant than the Fe/MnO₂ ratio.

The present work investigates the effect of using of tailings, obtained after flotation of slag at the Altonorte Foundry Plant, on the dissolution of Mn from marine nodules. A report by SERNAGEOMIN [17] indicates that the production of copper concentrate in Chile has been increasing steadily, and is expected to almost double by 2026 from its 2014 level, from 3.9 to 5.4 million tons. For every ton of Cu concentrate obtained by flotation, 151 tons of tailings are generated [18], which are disposed of in tailing dams and have significant impacts on the environment [19]. Consequently, it is necessary to find new uses for tailings with the application of more environmentally friendly hydrometallurgical techniques [20]. This results in an attractive proposal given the quantities of waste generated in the country by flotation, providing an added value for this material while introducing a new initiative in the context of the need to overcome stagnation in the mining sector [21].

2. Materials and Methods

2.1. Manganese Nodule Sample

The marine nodules used in this work were the same as those used in Toro et al. [11]. They were composed of 15.96% Mn and 0.45% Fe. Table 1 shows the chemical composition. The sample material was analyzed with a Bruker®M4-Tornado μ-FRX tabletop device (Fremont, CA, USA). The μ-XRF data shows that the nodules were composed of fragments of preexisting nodules that formed their nuclei, with concentric layers that precipitated around the nuclei in later stages.

Table 1. Chemical analysis (in the form of oxides) of manganese nodules.

Component	MgO	Al ₂ O ₃	SiO ₂	P ₂ O ₅	SO ₃	K ₂ O	CaO	TiO ₂	MnO ₂	Fe ₂ O ₃
Weight (%)	3.54	3.69	2.97	7.20	1.17	0.33	22.48	1.07	29.85	26.02

2.2. Tailings

The sample of tailings used in this study was obtained after flotation of slag during the production of copper concentrate at the Altonorte Smelting Plant. The methods used to determine the chemical and mineralogical composition of the tailings were the same as those used to determine marine nodule content. Chemical species were determined by QEMSCAN. Several iron-containing phases were present, while the Fe content was estimated at 41.9%. Table 2 shows the mineralogical composition of the tailings. As the Fe was mainly in the form of magnetite, the most appropriate method of extraction was the same as that used in Toro et al. [11].

Table 2. Mineralogical composition of tailings, as determined by QEMSCAN.

Mineral	Amount % (w/w)
Chalcopyrite/Bornite ($\text{CuFeS}_2/\text{Cu}_5\text{FeS}_4$)	0.47
Tennantite/Tetrahedrite ($\text{Cu}_{12}\text{As}_4\text{S}_{13}/\text{Cu}_{12}\text{Sb}_4\text{S}_{13}$)	0.03
Other Cu Minerals	0.63
Cu–Fe Hydroxides	0.94
Pyrite (FeS_2)	0.12
Magnetite (Fe_3O_4)	58.52
Specular Hematite (Fe_2O_3)	0.89
Hematite (Fe_2O_3)	4.47
Ilmenite/Titanite/Rutile ($\text{FeTiO}_3/\text{CaTiSiO}_5/\text{TiO}_2$)	0.04
Siderite (FeCO_3)	0.22
Chlorite/Biotite ($\text{Mg}_3(\text{Si})_4\text{O}_{10}(\text{OH})_2(\text{Mg})_3(\text{OH})_6/\text{K}(\text{Mg})_3\text{AlSi}_3\text{O}_{10}(\text{OH})_2$)	3.13
Other Phyllosilicates	11.61
Fayalite (Fe_2SiO_4)	4.59
Dicalcium Silicate (Ca_2SiO_4)	8.30
Kirschsteinite (CaFeSiO_4)	3.40
Forsterite (Mg_2SiO_4)	2.30
Barite (BaSO_4)	0.08
Zinc Oxide (ZnO)	0.02
Lead Oxide (PbO)	0.01
Sulfate (SO_4)	0.20
Others	0.03
Total	100.00

2.3. Reagents Used—Leaching Parameters

The sulfuric acid used for the leaching tests was grade P.A., with 95%–97% purity, a density of 1.84 kg/L, and a molecular weight of 98.8 g/mol. The leaching tests were carried out in a 50 mL glass reactor with a 0.01 solid/liquid ratio. A total of 200 mg of Mn nodules were maintained in suspension with the use of a 5-position magnetic stirrer (IKA ROS, CEP 13087-534, Campinas, Brazil) at a speed of 600 rpm. The tests were conducted at a room temperature of 25 °C, while the parameters studied were additives, particle size, and leaching time. Also, the tests were performed in duplicate, measurements (or analyses) were carried on 5 mL of undiluted samples using atomic absorption spectrometry with a coefficient of variation $\leq 5\%$ and a relative error between 5% to 10%.

2.4. Experimental Design

The effect of the independent variables on the extraction rate of Mn from manganese nodules was studied using the response surface method [22,23], which helped in understanding and optimizing the response by refining the determinations of relevant factors using the model. An experiment was designed involving three factors that could influence the response variable, and with three levels for each factor for a total of 27 experimental tests (Table 3), the purpose of which was to study the effects of H_2SO_4 concentration, particle size, and time on the dependent variable. Minitab 18 software was used for modeling and experimental design, providing the same analytical approach as used in Toro et al. [11].

Table 3. Experimental configuration and Mn extraction data.

Exp. No.	Time (min)	Sieve Fraction (Tyler Mesh)	Particle Size (μm)	Sulfuric Acid Conc. (mol/L)	Mn Extraction (%)
1	10	−320 + 400	−47 + 38	0.1	8.12
2	20	−100 + 140	−150 + 106	0.5	29.10
3	20	−320 + 400	−47 + 38	1	55.51
4	30	−320 + 400	−47 + 38	1	71.00
5	10	−200 + 270	−75 + 53	0.5	19.12
6	20	−100 + 140	−150 + 106	0.1	7.63
7	30	−100 + 140	−150 + 106	1	49.8
8	30	−200 + 270	−75 + 53	0.1	17.79
9	10	−100 + 140	−150 + 106	0.5	13.98
10	10	−100 + 140	−150 + 106	1	41.22
11	20	−320 + 400	−47 + 38	0.5	52.51
12	30	−100 + 140	−150 + 106	0.1	10.89
13	20	−320 + 400	−47 + 38	0.1	19.12
14	10	−100 + 140	−150 + 106	0.1	5.24
15	10	−320 + 400	−47 + 38	1	46.23
16	10	−200 + 270	−75 + 53	0.1	9.54
17	20	−200 + 270	−75 + 53	0.1	11.11
18	20	−200 + 270	−75 + 53	0.5	29.41
19	30	−320 + 400	−47 + 38	0.1	19.43
20	30	−320 + 400	−47 + 38	0.5	59.16
21	10	−200 + 270	−75 + 53	1	46.77
22	20	−200 + 270	−75 + 53	1	54.00
23	20	−100 + 140	−150 + 106	1	47.24
24	30	−200 + 270	−75 + 53	0.5	33.67
25	10	−320 + 400	−47 + 38	0.5	38.23
26	30	−200 + 270	−75 + 53	1	63.50
27	30	−100 + 140	−150 + 106	0.5	30.00

The response variable can be expressed as showed in Equation (1):

$$Y = (\text{overall constant}) + (\text{linear effects}) + (\text{interaction effects}) + (\text{curvature effects}) \quad (1)$$

Table 4 shows the ranges for values of the parameters used for the experimental design.

Table 4. Experimental conditions.

Parameters/Values	Low	Medium	High
Sieve fraction (Tyler mesh)	−100 + 140	−200 + 270	−320 + 400
Particle size (μm)	−150 + 106	−75 + 53	−47 + 38
Time (in min)	10	20	30
H ₂ SO ₄ (mol/L)	0.1	0.5	1

The levels of the factors are coded as (−1, 0, 1), where each number represents a particular value of the factor, with (−1) as the lowest value, (0) as the intermediate, and (1) as the highest. Equation (2) is used to transform a real value (Z_i) into a coded value (X_i) according to the experimental design:

$$X_i = \frac{Z_i - \frac{Z_{\text{high}} + Z_{\text{low}}}{2}}{\frac{Z_{\text{high}} - Z_{\text{low}}}{2}} \quad (2)$$

where Z_{high} and Z_{low} are, respectively, the highest and lowest values of a variable [22].

The statistics used to determine whether the model can adequately describe the extraction of Mn from marine nodules are similar with those used in the study of Toro et al. [11].

2.5. Effect of Stirring Speed

The effect of particle size was evaluated by Toro et al. [11]. It was concluded that this variable did not significantly influence the manganese solutions. Consequently, the present work assessed the effect of agitation speed on Mn dissolution kinetics.

This investigation determined the effect of increasing agitation speed (200, 400, 600, 800, and 1000 rpm) on leaching manganese nodules, using a particle size of $-75 + 53 \mu\text{m}$, $\text{MnO}_2/\text{Fe}_2\text{O}_3$ ratio of 1, leaching solution volume of 20 mL, 1 mol/L sulfuric acid, and room temperature (25 °C).

2.6. Effect of the $\text{MnO}_2/\text{Fe}_2\text{O}_3$ Ratio

The present study evaluated the effect of the $\text{MnO}_2/\text{Fe}_2\text{O}_3$ ratio on leaching time with the use of tailings, using a particle size of $-75 + 53 \mu\text{m}$, agitation speed of 600 rpm, leaching solution volume of 20 mL, 1 mol/L sulfuric acid, and room temperature (25 °C).

3. Results and Discussion

3.1. Effect of Variables

Based on the information obtained from the ANOVA analysis (Table 5), the linear effects of particle size, H_2SO_4 , and time contribute greatly to explaining the experimental model, as shown in the contour plots (Figures 1 and 2), while there was no significant effect of any of the curvatures and interactions of the variables considered ($p \gg 0.05$) on the manganese extraction rate.

Table 5. ANOVA of the Mn extraction rate.

Source	F-Value	p-Value
Regression	32.13	0.000
Time	27.12	0.000
Particle size	30.39	0.000
Sulfuric acid	226.50	0.000
Time × Time	0.43	0.522
Particle size × Particle size	0.67	0.423
Sulfuric acid × Sulfuric acid	0.39	0.542
Time × Particle size	1.81	0.196
Time × Sulfuric acid	1.57	0.228
Particle size × Sulfuric acid	0.34	0.568

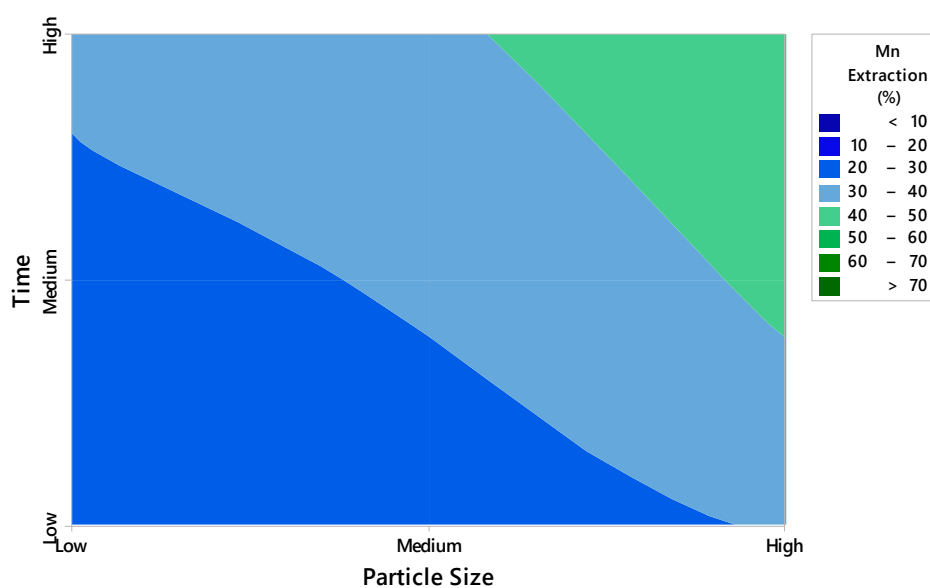


Figure 1. Experimental contour plot of Mn extraction (25 °C; $-150 + 106$, $-75 + 53$, $-47 + 38 \mu\text{m}$ particle size; 10, 20, 30 min leaching time).

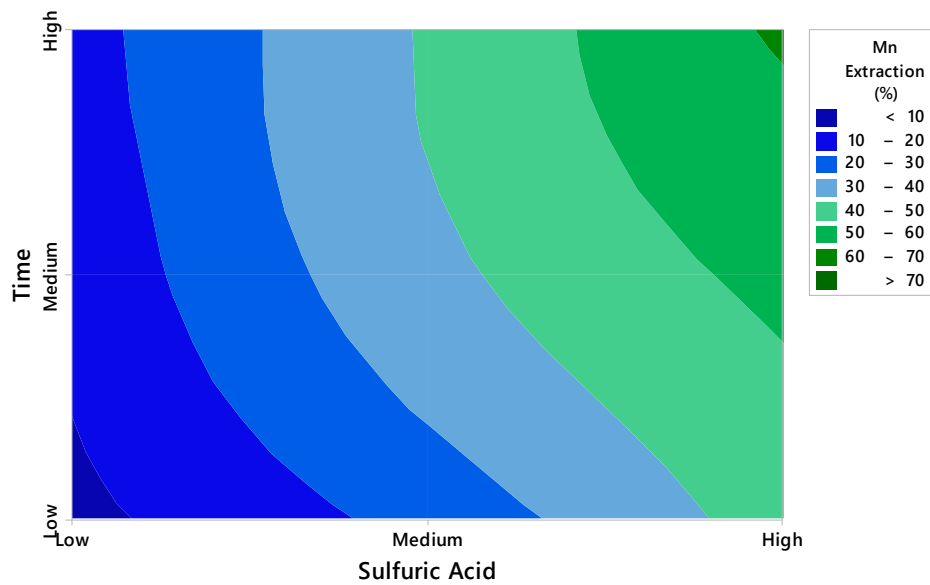


Figure 2. Experimental contour plot of Mn extraction (25 °C; 10, 20, 30 min leaching time; 0.1, 0.5, 1 mol/L H₂SO₄).

Figures 3–5 show that the linear effects of time, particle size, and H₂SO₄ concentration had the most significant impact on Mn extraction rates.

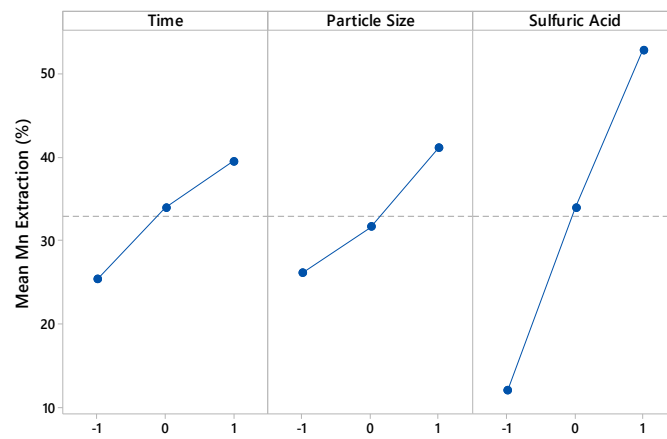


Figure 3. Linear effect plot for Mn extraction.

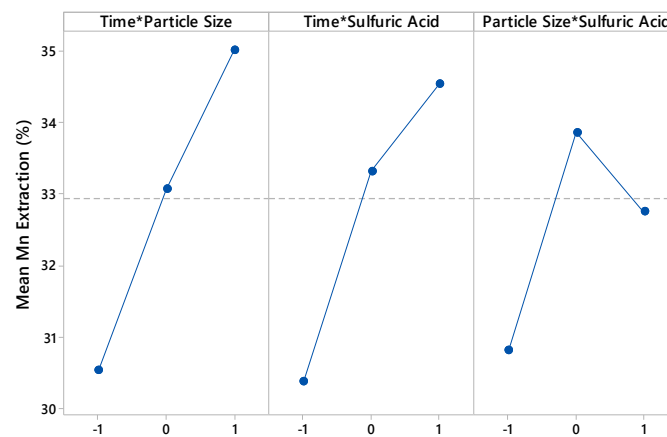


Figure 4. Interaction effect plot for Mn extraction.

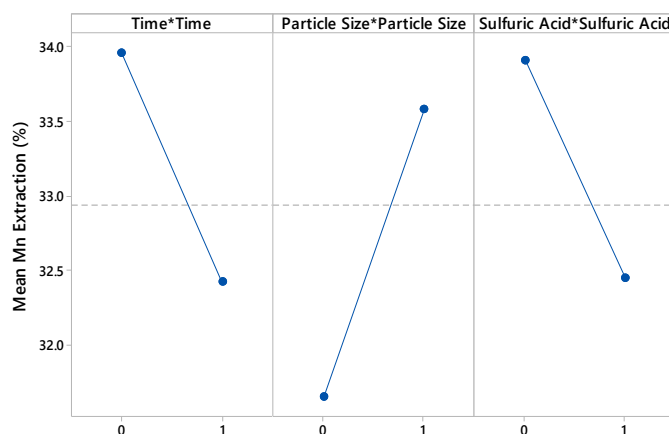


Figure 5. Curvature effect plot for Mn extraction.

After eliminating non-significant coefficients, the model developed to predict ore extraction over the range of experimental conditions is presented in Equation (3).

$$\text{Mn Extraction} = 0.3294 + 0.0704x_1 + 0.0746x_2 + 0.2036x_3 \quad (3)$$

where x_1 , x_2 , and x_3 are coded variables representing time, particle size, and H_2SO_4 concentration, respectively.

Figure 6 shows the order of adding parameters to the model, graphically showing the contribution to explaining the variability of each new parameter.

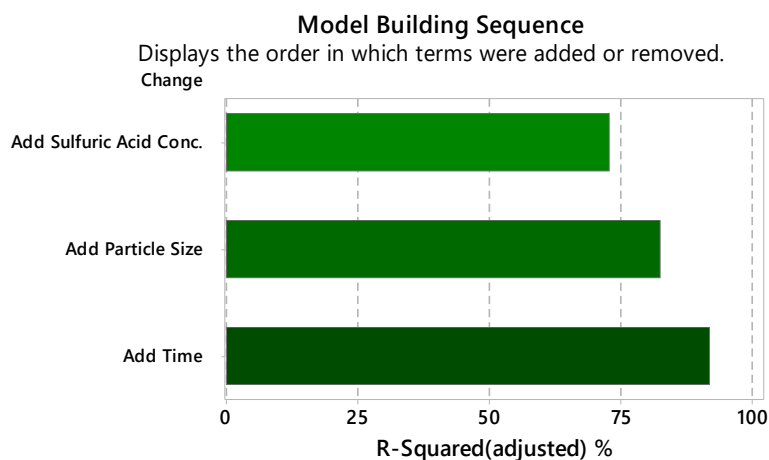


Figure 6. Construction sequence of the model.

The ANOVA indicates that the model adequately represents Mn extraction under the range of established parameters. The model does not require adjustment and is validated by the value of R^2 (0.9275) (Figure 7). The ANOVA shows that the effect of the indicated factors on manganese extraction is $F_{\text{regression}} (98.07) > F_{\text{Table}}$, at the 95% confidence level $F_{4,22} (2.8167)$.



92.75% of the variation in Y can be explained by the regression model.

Figure 7. Statistic R^2 (% of variation explained by the model).

Additionally, the p-value (Figure 8) of the model represented by the Equation (3) indicates that the model is statistically significant.

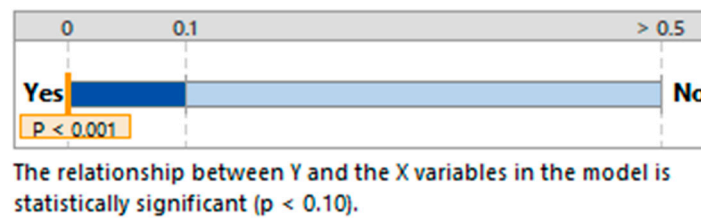


Figure 8. Statistic p.

In favor of the above analysis, the number of parameters plus the constant of the regression does not differ greatly from Mallows' Cp statistic, which indicates that the model is relatively accurate and does not present a bias in estimating the true coefficients of the regression, in addition to making predictions with an acceptable margin of error ($R_{pred} = 90.02\%$).

The data points from the normality test applied to the residuals resulting from the regression in Figure 9 are relatively close to the adjusted normal distribution line, and the p-value of the test is greater than the level of significance of 0.05, so it is not possible to reject the assumption of the regression model, that the residuals are distributed normally.

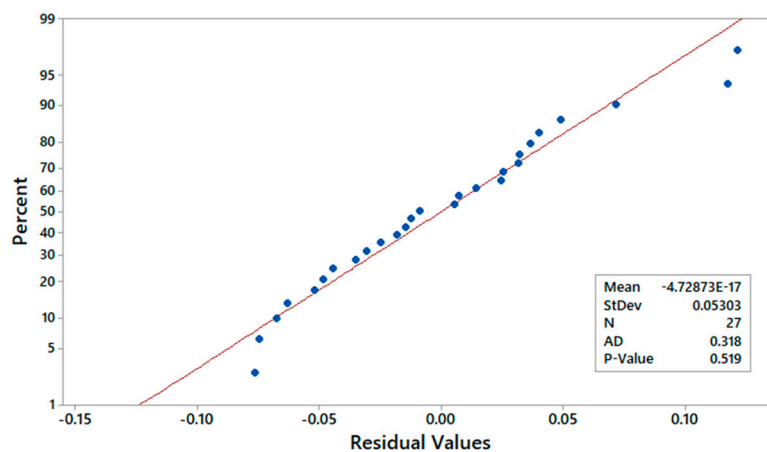


Figure 9. Probability plot of residual values.

Figure 10 shows that residuals do not correlate, indicating that they are independent of each other as there are no obvious trends or patterns.

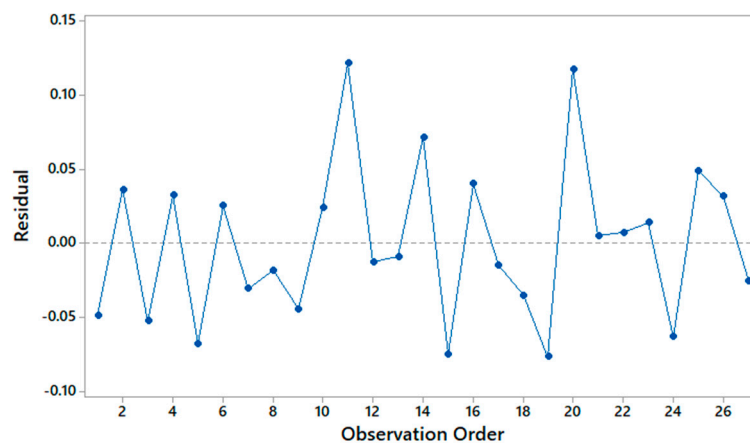


Figure 10. Residuals according to observations.

The response surface graphs in Figure 11A show that manganese extraction increases with time and particle size, while Figure 11B shows, graphically, that the effect of the variable H_2SO_4 concentration is greater than that of time, resulting in a more significant increase in extraction only when the acid concentration increases. The effect described above occurs analogously with variations in particle size and sulfuric acid concentration (Figure 11C).

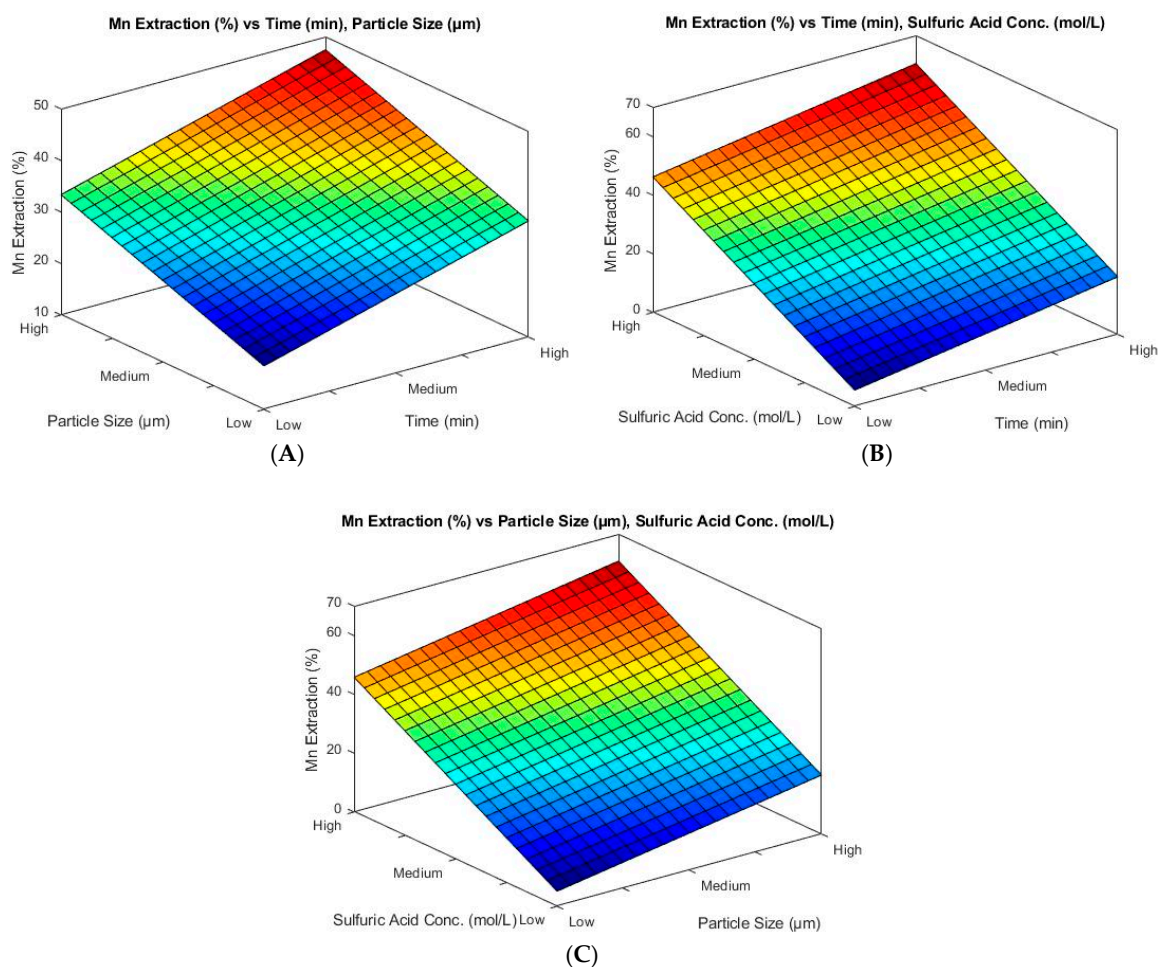


Figure 11. Response surface of the independent variables of time and particle size (A); time and H_2SO_4 concentration (B); and particle size and H_2SO_4 concentration (C) on the dependent variable of Mn extraction.

3.2. Effect of Agitation Speed

In Figure 12, it can be seen that higher Mn extraction rates are obtained at higher agitation speeds. In this study, the highest rate of 69% was obtained with a speed of 600 rpm and a time of 30 min. The extraction rate was lower at 800 and 1000 rpm because, at these speeds, some of the mineral breaks away and adheres to the reactor wall. Jiang et al. [13] had a similar observation at the speed of 1000 rpm. The extraction rate, at 400 rpm (58%), was not significantly different from what was obtained at 600 rpm, while at a low speed of 200 rpm, the Mn extraction rate was only 35% at 30 min. It was observed that not all the particles were in suspension at a stirring speed of 200 rpm, which explains why the extraction rate was so much lower. This is consistent with what Velásquez et al. [16] found in a study of leaching chalcopyrite mineral in chlorinated media. These authors concluded that agitation speed was not the most important factor in determining extraction rates as long as all the particles of the system are kept in suspension.

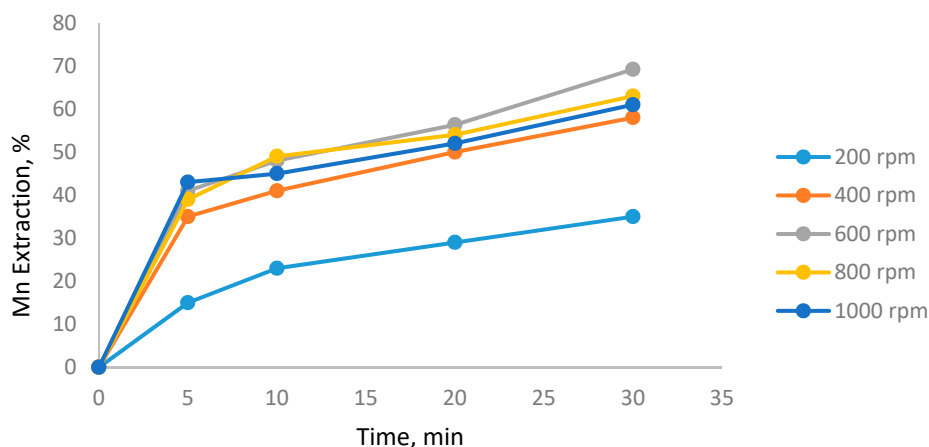


Figure 12. Effect of stirring speed on manganese extraction (25 °C, $\text{MnO}_2/\text{Fe}_2\text{O}_3$ ratio of 1, $-75 + 53 \mu\text{m}$, 1 mol/L H_2SO_4).

3.3. Effect of the $\text{MnO}_2/\text{Fe}_2\text{O}_3$ Ratio

The results presented in Figure 13 show the benefit of operating at high concentrations of reducing agent (Fe) in terms of shortening the dissolution time. The highest Mn extraction of 77% was obtained after 40 min with an $\text{MnO}_2/\text{Fe}_2\text{O}_3$ ratio of 1/2. Notably, at this $\text{MnO}_2/\text{Fe}_2\text{O}_3$ ratio, the leaching time required to reach a 70% extraction rate has been shortened significantly, while 67% extraction was reached in 5 min. However, the extraction graph shows asymptotic behavior, with no significant increase in the extraction rate vs. time. It can be observed that the extraction rate for 30 min with an $\text{MnO}_2/\text{Fe}_2\text{O}_3$ ratio of 1/1 is close to that obtained with a ratio of 1/2. However, the differences in dissolution rates are more significant for short periods of time (between 5 and 20 min). Finally, the Mn extraction rate was lower (maximum of 47% in 40 min) with an $\text{MnO}_2/\text{Fe}_2\text{O}_3$ ratio of 2/1 than with the ratios mentioned above. The tests conducted in this investigation were in pH ranges between -2 to 0.1 , and potentials from -0.4 to 1.4 V, because the presence of Fe_2O_3 maintains the regeneration of ferrous ions, which results in high levels of ferrous ion concentration and activity, favoring the dissolution of Mn and avoiding the formation of precipitates through oxidation–reduction reactions.

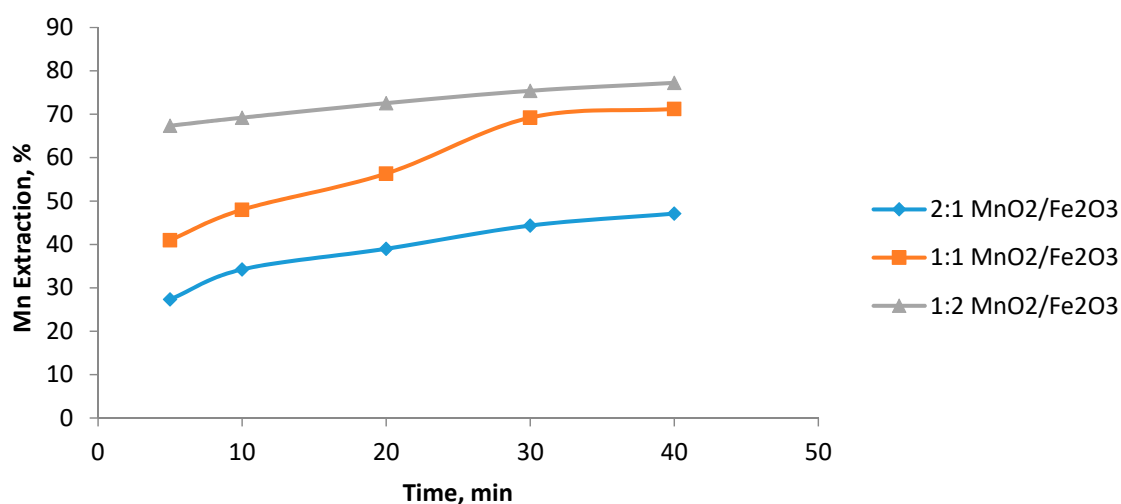


Figure 13. Effect of the $\text{MnO}_2/\text{Fe}_2\text{O}_3$ ratio on manganese extraction (25 °C, $-75 + 53 \mu\text{m}$, 1 mol/L H_2SO_4).

Table 6 compares the results using Fe present in slag and tailings as a reducing agent for Mn dissolution under the same operational conditions. In both cases, dissolution over a short period of time (5 min) immediately reached values close to 70%, with almost identical levels in the two investigations.

However, better results were obtained at 40 min using tailings instead of slag, although the difference is small (7%). This is possibly due to the presence of 13.07% Cu in the slag, which consumes protons. However, this issue requires additional study, since the reactivity of Cu in acid media is associated with slag mineralogy, and the presence of high silica often results in gel formation when leaching is carried out in low pH values [24]. In addition, the tailings are more reactive since they are derived from flotation, and have been attacked by chemicals, resulting in exposure of their surface [25]. These results are promising for future hydrometallurgical studies to investigate the use of slag and tailings as reducing agents for manganese ores. In future studies, it is proposed that this research be continued under the same operating parameters and by applying elemental iron (Fe^0) to determine if it is possible to achieve better results within short periods of time (5 min). In addition, when slag and tailings are used for Mn reduction, the effect of temperature should be evaluated to determine if it is possible to obtain 100% extraction in short periods of time. Finally, an optimal $\text{MnO}_2/\text{Fe}_2\text{O}_3$ ratio must be found.

Table 6. Comparison of the experimental results.

Experimental Conditions	Toro et al. [11] (2018)	Present Investigation
Temperature ($^{\circ}\text{C}$)	25	25
Particle size of Mn nodules and slag/tailings (μm)	$-75 + 53$	$-75 + 53$
H_2SO_4 concentration (mol/L)	1	1
$\text{MnO}_2/\text{Fe}_2\text{O}_3$ ratio	1/2	1/2
Mn dissolution rate at 5 min (%)	68	67
Mn dissolution rate at 40 min (%)	70	77

For the recovery of Mn from the solution, the use of zerovalent iron (ZVI) is proposed. In a study by Bartzas et al. [26], the performance of a Fe^0 permeable reactive barrier (PRB) was evaluated for the treatment of acid leachates, where it was observed that metals, such as aluminum, manganese, nickel, cobalt, and zinc, were mainly removed from solution, as metal hydroxides, by precipitation. This can be an attractive proposal because zerovalent iron is a cheap byproduct obtained from the metal finishing industries.

Table 6 shows a comparison of the experimental results of Mn extraction from marine nodules with the use of slag and slag flotation tailings.

4. Conclusions

This investigation presents the results of dissolving Mn from marine nodules in an acid medium at room temperature ($25\text{ }^{\circ}\text{C}$) with the use of tailings obtained from flotations of smelter slag. The Fe present in the tailings proved to be a good reducing agent, increasing MnO_2 dissolution kinetics. The findings of this study are as follows:

- (1) The ANOVA test indicates that sulfuric acid is the factor that has the greatest impact on manganese extraction under the studied conditions.
- (2) The manganese dissolution rate was generally higher when tailings were used instead of slag, possibly because tailings are more reactive to leaching.
- (3) Increase of the agitation speed did not significantly increase Mn extraction.
- (4) The highest Mn extraction rate of 77% was obtained at an $\text{MnO}_2/\text{Fe}_2\text{O}_3$ ratio 0.5, 1 mol/L H_2SO_4 , particle size of $-47 + 38\ \mu\text{m}$, and leaching time of 40 min.

In future work, the leaching of marine nodules should be studied using different Fe reducing agents but under the same operational conditions. It is also necessary to determine the optimal $\text{MnO}_2/\text{Fe}_2\text{O}_3$ ratio that improves dissolution of Mn. In addition, SEM studies need to be carried out on the tailings and manganese nodules after leaching, in order to observe their morphology and determine the possible formation of any iron precipitates.

Author Contributions: N.T. and M.S. contributed in the methodology, conceived and designed the experiments; analyzed the data and wrote paper, J.C. performed the experiments, F.H. contributed with resources and R.A. contributed with review and editing.

Funding: This research received no external funding.

Acknowledgments: The authors are grateful for the contribution of the Scientific Equipment Unit MAINI of the Universidad Católica del Norte for aiding in generating data by automated electronic microscopy QEMSCAN® and for facilitating the chemical analysis of the solutions. We are also grateful to the Altonorte Mining Company for supporting this research and providing slag for this study, and we thank to Marina Vargas Aleuy and María Barraza Bustos of the Universidad Católica del Norte for supporting the experimental tests. This research was supported by FCAC 2018-UCN.

Conflicts of Interest: The authors declare they have no conflict of interest.

References

1. Marino, E.; González, F.J.; Somoza, L.; Lunar, R.; Ortega, L.; Vázquez, J.T.; Reyes, J.; Bellido, E. Strategic and rare elements in Cretaceous-Cenozoic cobalt-rich ferromanganese crusts from seamounts in the Canary Island Seamount Province (northeastern tropical Atlantic). *Ore Geol. Rev.* **2017**, *87*, 41–61. [[CrossRef](#)]
2. Nishi, K.; Usui, A.; Nakasato, Y.; Yasuda, H. Formation age of the dual structure and environmental change recorded in hydrogenetic ferromanganese crusts from Northwest and Central Pacific seamounts. *Ore Geol. Rev.* **2017**, *87*, 62–70. [[CrossRef](#)]
3. Konstantinova, N.; Cherkashov, G.; Hein, J.R.; Mirão, J.; Dias, L.; Madureira, P.; Kuznetsov, V.; Maksimov, F. Composition and characteristics of the ferromanganese crusts from the western Arctic Ocean. *Ore Geol. Rev.* **2017**, *87*, 88–99. [[CrossRef](#)]
4. Usui, A.; Nishi, K.; Sato, H.; Nakasato, Y.; Thornton, B.; Kashiwabara, T. Continuous growth of hydrogenetic ferromanganese crusts since 17 Myr ago on Takuyo-Daigo Seamount, NW Pacific, at water depths of 800–5500 m. *Ore Geol. Rev.* **2017**, *87*, 71–87. [[CrossRef](#)]
5. Josso, P.; Pelleter, E.; Pourret, O.; Fouquet, Y.; Etoubleau, J.; Cheron, S.; Bollinger, C. A new discrimination scheme for oceanic ferromanganese deposits using high field strength and rare earth elements. *Ore Geol. Rev.* **2017**, *87*, 3–15. [[CrossRef](#)]
6. Senanayake, G. Acid leaching of metals from deep-sea manganese nodules—A critical review of fundamentals and applications. *Miner. Eng.* **2011**, *24*, 1379–1396. [[CrossRef](#)]
7. Randhawa, N.S.; Hait, J.; Jana, R.K. A brief overview on manganese nodules processing signifying the detail in the Indian context highlighting the international scenario. *Hydrometallurgy* **2016**, *165*, 166–181. [[CrossRef](#)]
8. Kanungo, S.B. Rate process of the reduction leaching of manganese nodules in dilute HCl in presence of pyrite. Part I. Dissolution behaviour of iron and sulphur species during leaching. *Hydrometallurgy* **1999**, *52*, 313–330. [[CrossRef](#)]
9. Kanungo, S.B. Rate process of the reduction leaching of manganese nodules in dilute HCl in presence of pyrite. Part II: leaching behavior of manganese. *Hydrometallurgy* **1999**, *52*, 331–347. [[CrossRef](#)]
10. Zakeri, A.; Bafghi, M.S.; Shahriari, S.; Das, S.C.; Sahoo, P.K.; Rao, P.K. Dissolution kinetics of manganese dioxide ore in sulfuric acid in the presence of ferrous ion. *Hydrometallurgy* **2007**, *8*, 22–27.
11. Toro, N.; Herrera, N.; Castillo, J.; Torres, C.; Sepúlveda, R. Initial Investigation into the Leaching of Manganese from Nodules at Room Temperature with the Use of Sulfuric Acid and the Addition of Foundry Slag—Part I. *Minerals* **2018**, *8*, 565. [[CrossRef](#)]
12. Bafghi, M.S.; Zakeri, A.; Ghasemi, Z.; Adeli, M. Reductive dissolution of manganese ore in sulfuric acid in the presence of iron metal. *Hydrometallurgy* **2008**, *90*, 207–212. [[CrossRef](#)]
13. Jiang, T.; Yang, Y.; Huang, Z.; Zhang, B.; Qiu, G. Leaching kinetics of pyrolusite from manganese-silver ores in the presence of hydrogen peroxide. *Hydrometallurgy* **2004**, *72*, 129–138. [[CrossRef](#)]
14. Su, H.; Liu, H.; Wang, F.; Lü, X.; Wen, Y. Kinetics of reductive leaching of low-grade pyrolusite with molasses alcohol wastewater in H₂SO₄. *Chin. J. Chem. Eng.* **2010**, *18*, 730–735. [[CrossRef](#)]
15. Zhang, Y.; You, Z.; Li, G.; Jiang, T. Manganese extraction by sulfur-based reduction roasting-acid leaching from low-grade manganese oxide ores. *Hydrometallurgy* **2013**, *133*, 126–132. [[CrossRef](#)]
16. Velásquez Yévenes, L.; Miki, H.; Nicol, M. The dissolution of chalcopyrite in chloride solutions: Part 2: Effect of various parameters on the rate. *Hydrometallurgy* **2010**, *103*, 80–85. [[CrossRef](#)]
17. SERNAGEOMIN. *Anuario de la minería de Chile 2017*; SERNAGEOMIN: Santiago, Chile, 2017.

18. COCHILCO. *Sulfuros primarios: desafíos y oportunidades I Comisión Chilena del Cobre*; COCHILCO: Santiago, Chile, 2017.
19. Oyarzun, R.; Oyarzún, J.; Lillo, J.; Maturana, H.; Higuera, P. Mineral deposits and Cu-Zn-As dispersion-contamination in stream sediments from the semiarid Coquimbo Region, Chile. *Environ. Geol.* **2007**, *53*, 283–294. [[CrossRef](#)]
20. Baba, A.A.; Ayinla, K.I.; Adekola, F.A.; Ghosh, M.K.; Ayanda, O.S.; Bale, R.B.; Sheik, A.R.; Pradhan, S.R. A Review on Novel Techniques for Chalcopyrite Ore Processing. *Int. J. Min. Eng. Miner. Process.* **2012**, *1*, 1–16. [[CrossRef](#)]
21. Centro de Estudios del Cobre y la Minería (CESCO). Available online: <http://www.cesco.cl/en/home-en/> (accessed on 11 May 2019).
22. Montgomery, D.C. *Design and Analysis of Experiments*; Wiley: Hoboken, NJ, USA, 2012.
23. Bezerra, M.A.; Santelli, R.E.; Oliveira, E.P.; Villar, L.S.; Escalera, L.A. Response surface methodology (RSM) as a tool for optimization in analytical chemistry. *Talanta* **2008**, *76*, 965–977. [[CrossRef](#)] [[PubMed](#)]
24. Komnitsas, K.; Zaharaki, D.; Perdikatsis, V. Effect of synthesis parameters on the compressive strength of low-calcium ferronickel slag inorganic polymers. *J. Hazard. Mater.* **2009**, *161*, 760–768. [[CrossRef](#)] [[PubMed](#)]
25. Komnitsas, K.; Manousaki, K.; Zaharaki, D. Assessment of reactivity of sulphidic tailings and river sludges. *Geochemistry Explor. Environ. Anal.* **2009**, *9*, 313–318. [[CrossRef](#)]
26. Bartzas, G.; Komnitsas, K.; Paspaliaris, I. Laboratory evaluation of Fe0 barriers to treat acidic leachates. *Miner. Eng.* **2006**, *19*, 505–514. [[CrossRef](#)]



© 2019 by the authors. Licensee MDPI, Basel, Switzerland. This article is an open access article distributed under the terms and conditions of the Creative Commons Attribution (CC BY) license (<http://creativecommons.org/licenses/by/4.0/>).